Plasma Physics Reports, Vol. 27, No. 12, 2001, pp. 1025–1031. Translated from Fizika Plazmy, Vol. 27, No. 12, 2001, pp. 1085–1092.

NONIDEAL PLASMA

Phase Transition in Superdense Hydrogen and Deuterium

M. Bonitz*, I. A. Mulenko, E. N. Oleynikova**, V. S. Filinov***, V. E. Fortov***, and A. L. Khomkin****

**Faculty of Physics, University of Rostock, Germany*

***Associated Institute for High Temperatures, Russian Academy of Sciences, Izhorskaya ul. 13/19, Moscow, 127412 Russia*

****Institute for High Energy Densities, Associated Institute for High Temperatures, Russian Academy of Sciences, Izhorskaya ul. 13/19, Moscow, 127412 Russia*

Received May 11, 2001; in final form, June 25, 2001

Abstract—Results are presented from numerical simulations of the thermodynamic properties of superdense hydrogen and deuterium plasmas by the Monte Carlo method and from calculations by a multicomponent chemical model. The results obtained reveal the anomalous behavior of the thermodynamic functions and composition of molecular gas plasmas in the submegabar and megabar pressure ranges. Such behavior is interpreted as a dissociative phase transition. The results of calculations by the chemical model are compared with the experimental data on the equation of state and conductivity of hydrogen and deuterium plasmas. © *2001 MAIK "Nauka/Interperiodica".*

1. INTRODUCTION

Experiments on the thermodynamic and transport properties of dense hydrogen and deuterium plasmas [1–3] revealed the unusual behavior of the conductivity of hydrogen [1, 2] and the shock adiabat of deuterium [3] in the megabar pressure range. The results of [1, 2] show that, in the pressure range $P = 10^5$–2×10^6 atm, the conductivity of a hydrogen plasma increases rapidly (by nearly five orders of magnitude) as the pressure varies within relatively narrow (~40–50%) limits. The measurements were carried out in the temperature range $(4.5–10) \times 10^3$ K. From a theoretical standpoint, the behavior of the shock adiabat of deuterium measured in [3], which demonstrates a sharp change in the deuterium density in the megabar pressure range at densities of 0.5–1 g/cm^3, also seems unusual.

Such behavior of the thermodynamic and transport properties of a plasma indicates the possible existence of phase transitions of the first kind that are accompanied by a rapid or even abrupt change in the plasma composition and density. The occurrence of phase transitions in a low-temperature plasma was first hypothesized in [4]. Later, attempts were made to study the parameters of plasma phase transition, primary attention being focused on the Coulomb interaction [5–7].

In this paper, the behavior of the thermodynamic properties of hydrogen and deuterium plasmas in the above pressure and density ranges is studied comparatively by the Monte Carlo quantum method [8, 9] for hydrogen and by using the chemical model of a multicomponent nonideal plasma [10] for hydrogen and deuterium. It is shown that the experimentally observed behavior of the conductivity of dense hydrogen and the deuterium shock adiabat can be explained by the existence of a new phase transition occurring in dense hydrogen and deuterium. The critical transition temperature and the phase coexistence curve are found. The electric conductivity of hydrogen and the deuterium shock adiabat are calculated and compared with the experimental data.

2. NUMERICAL SIMULATIONS

For the numerical simulations of a hydrogen plasma, we use an original efficient modification of the Monte Carlo quantum method elaborated in [8, 9]. The modified method allows us to study dense degenerate plasmas over a wide range of densities and temperatures. We consider a system consisting of 50 electrons and 50 hydrogen ions in a cell with periodic boundary conditions.

Thermodynamic quantities are calculated as derivatives of the logarithm of the statistical sum [11]. The statistical sum of a quantum system is expressed through the density matrix. An exact expression for the density matrix of a quantum system at low temperatures is still unknown. To approximate this sum, we can represent it in the form of integrals over trajectories [11]. The spin variables are taken into account by the spin part of the density matrix, whereas the permutation operator acting on the spatial and spin coordinates of electrons allows for exchange effects. The sum is taken over all permutations with a given parity. For Fermi particles, this sum contains positive and negative terms, which poses the well-known "problem of signs."

1063-780X/01/2712-1025$21.00

In the developed approach [8, 9], the density matrix is described by the expression

$$\rho_s(q, [r], \beta) = C^s_{N_e} e^{-\beta U(q, [r], \beta)} \prod_{l=1}^{n} \prod_{p=1}^{N_e} \Phi^l_{pp} \det \left| \Psi^{n,l}_{ab} \right|_s. \quad (1)$$

The matrix does not contain the alternating-sign sum over permutations in the explicit form. The exchange effects are accounted for in the determinant of the exchange density matrix:

$$\left\| \Psi^{n,l}_{ab} \right\|_s \equiv \left\| \exp\left(-\frac{\pi}{\Delta\lambda_e^2} \left| (\mathbf{r}_a - \mathbf{r}_b) + \mathbf{y}^n_a \right|^2 \right) \right\|_s. \quad (2)$$

In formulas (1) and (2), we introduced the following notation: $U(q, [r], \beta)$ is the sum of Kelbg potentials, $\Phi^l_{pp} \equiv \exp[-\pi \left| \xi^{(l)}_p \right|^2]$, $\boldsymbol{\xi}^{[l]}_p$ are the dimensionless vectors connecting the nearest peaks of trajectories, $C^l_{pt} = \frac{(r^l_{pt} | y^l_{pt})}{2 |r^l_{pt}|}$, $\mathbf{y}^l_{pt} \equiv \mathbf{y}^l_p - \mathbf{y}^n_t$, $\mathbf{y}^n_a = \Delta\lambda_e \sum_{k=1}^{n} \boldsymbol{\xi}^{(k)}_a$, $r^l_{pt} \equiv r_{pt} + y^l_{pt}$, $\Delta\lambda_a^2 = \frac{2\pi\hbar^2\Delta\beta}{m_a}$, $\Delta\beta$ is the increment of the modulus of the canonic distribution, the $(\ldots|\ldots)$ bracket denotes the scalar product, and m_a is the mass of particles of the a species.

The summation over spin variables results in a block structure of the exchange density matrix for electrons with the same spin projections. The important advantage of expression (2) is that the sum over permutations is written in the form of a determinant that can be easily calculated by the conventional methods of linear algebra.

Using the Monte Carlo quantum method, we calculated the isotherms of a hydrogen plasma at temperatures of 10, 20, and 50 kK. The most interesting is the 10-kK isotherm. On this isotherm, there is a plasma density range in which a stable solution is absent. The plasma density changes abruptly from 10^{23} to 2×10^{24} cm^{-3} in a narrow pressure range. A similar situation also occurs for the 20-kK isotherm, but in a narrower density range. On the 50-kK isotherm, the instability domain is absent and the dependence of the pressure on the density is smooth up to densities of 10^{26} cm^{-3}. It was found that the range of the hydrogen plasma density with such a peculiar behavior of the equation of state nearly corresponds to the density range in which a sharp increase in the hydrogen plasma conductivity is observed [1, 2]. Unfortunately, it is still impossible to numerically calculate the conductivity of a hydrogen plasma. The Monte Carlo method allows one to calculate the thermodynamic functions but not transport coefficients, such as the electric conductivity. To calculate these coefficients, the method of molecular dynamics should be applied. In addition, when simulating using the Monte Carlo quantum method, a system of electrons and nuclei is used. Some electrons and nuclei form bound states. This can be seen from the form of the pair distribution functions [8]. However, there is no significant difference between free and bound electrons, so that it is difficult to determine the composition exactly.

In some sense, the simulations of hydrogen plasma thermodynamics can be regarded as an additional experiment on determining the equation of state of dense hydrogen, which is all the more useful because, in experiments [1–3], the temperature was not measured.

3. CHEMICAL MODEL

In [10], a chemical model of a nonideal plasma with allowance for chemical reactions was proposed. A distinctive feature of this model is the exclusion of a classically inaccessible phase space volume from the ensemble of free particles when calculating the corrections for their interaction. This correction appears because some states of the particles under consideration are bound and form particles of other species. The corrections for the interactions involving neutral particles are represented in terms of a power series in the density with allowance for all types of pair and three-body charge–neutral and neutral–neutral interactions [10]. The corresponding second and third virial coefficients associated with the interaction of free particles of different species were calculated in [12] by using the Hill pseudopotentials [13]. The Hill pseudopotentials describing the charge–neutral and neutral–neutral interactions were calculated using the (12-4) and (12-6) Lennard–Jones potentials, respectively, as the initial ones. The classically inaccessible phase space volume was taken into account in [14] when calculating the corrections for the interaction in an ensemble of free charged particles. The derived corrections to the thermodynamic functions differ substantially from the conventionally used Debye corrections. The thermodynamic quantities for a multicomponent, chemically reacting plasma of an arbitrary composition are represented in terms of a series in different interaction types. It is taken into account that the particles of different species interact with each other through the Coulomb and van der Waals forces with the parameters of the initial interaction potentials characteristic of a given pair of particles; the electron component is assumed to be weakly degenerate. For hydrogen and deuterium plasmas, six components (namely, e^-, A, A^+, A^-, A_2, and A_2^+, where A is the element symbol) were taken into account.

The expression for the free energy of a multicomponent plasma with allowance for the above-listed interactions and chemical reactions has the form (see notation in [10, 14])

$$F = -TV\Bigg\{\sum_{i=1}^{M} n_i \ln\frac{eZ_i}{n_i} - \sum_{i=1}^{M} n_i^2 B_{ii} - 2\sum_{i=1}^{M}\sum_{j=i+1}^{M} n_i n_j B_{ij} - \frac{1}{2}\sum_{i=1}^{M} n_i^3 C_{iii} - \frac{3}{2}\sum_{i=1}^{M}\sum_{j=i+1}^{M} n_i n_j^2 C_{ijj} - 3\sum_{i=1}^{M}\sum_{j=i+1}^{M}\sum_{k=j+1}^{M} n_i n_j n_k C_{ijk} - \frac{n_e^2\lambda_e^3}{2^{7/2}} + \sum_k n_k z_k^2\Bigg[\ln(1 + z_k^2(\alpha/2 + \alpha^2/4 - f_1)) - \frac{\alpha/6 + \alpha^2/8 - f_1/2}{1 + z_k^2(\alpha/2 + \alpha^2/4 - f_1)}\Bigg]\Bigg\}. \quad (3)$$

The equation of state and the set of chemical balance equations are written in the form

$$P = T\Bigg\{\sum_{i=1}^{M} n_i - \sum_i \frac{(\alpha/6 + \alpha^2/8 - f_1/2) n_i z_i^2}{1 + z_i^2(\alpha/2 + \alpha^2/4 - f_1)} + \sum_{i=1}^{M} n_i^2 B_{ii} + 2\sum_{i=1}^{M}\sum_{j=i+1}^{M} n_i n_j B_{ij} + \sum_{i=1}^{M} n_i^3 C_{iii} + 3\sum_{i=1}^{M}\sum_{j=i+1}^{M} n_i n_j^2 C_{ijj} + 6\sum_{i=1}^{M}\sum_{j=i+1}^{M}\sum_{k=j+1}^{M} n_i n_j n_k C_{ijk} + \frac{n_e^2\lambda_e^3}{2^{7/2}}\Bigg\}, \quad (4)$$

$$\frac{n_k}{n_l n_p} = \frac{Z_k}{Z_l Z_p}\exp\Bigg\{-\Bigg[2\sum_{i=1}^{M} n_i(B_{ki} - B_{li} - B_{pi}) + \frac{3}{2}\sum_{i=1}^{M} n_i^2(C_{kii} - C_{lii} - C_{pii}) + 3\sum_{i=1}^{M-1}\sum_{j=i+1}^{M} n_i n_j(C_{kij} - C_{lij} - C_{pij})\Bigg] - \ln[1 + z_l^2(\alpha/2 + \alpha^2/4 - f_1)] - \ln[1 + z_p^2(\alpha/2 + \alpha^2/4 - f_1)] + \ln[1 + z_k^2(\alpha/2 + \alpha^2/4 - f_1)] + \frac{n_e\lambda_e^3}{2^{5/2}}(\delta_{le} + \delta_{pe} - \delta_{ke})\Bigg\}. \quad (5)$$

In Eqs. (3)–(5), we introduce the following notation: $f_1(\alpha) = \frac{\pi\sqrt{6}}{24}\alpha + \frac{\sqrt{2\pi}\times 3^{1/6}\Gamma\left(\frac{1}{6}\right)}{48}\alpha^{5/3}$; α is the plasma coupling parameter (it is calculated through the activities); Z_k, z_k, and n_k are the statistical sum, charge number, and density of the particles of k species, respectively; T and V are the plasma temperature and volume; B_{ij} and C_{ijk} are the second and third virial coefficients; M is the total number of plasma particle species; λ_e is the thermal wavelength of electrons; and δ is the Kronecker symbol.

It should be stressed that taking into account the second and third virial coefficients in the free energy and in the equation of state allows one, in principle, to determine the parameters of the vapor–liquid phase transition.

4. COMPARISON OF ANALYTICAL RESULTS WITH NUMERICAL AND PHYSICAL EXPERIMENTS. DISSOCIATIVE PHASE TRANSITION

The described approaches were used to calculate the equilibrium properties of hydrogen and deuterium plasmas over a wide region of the phase diagram. A comparison of the results of calculations for both described approaches shows their satisfactory agreement in the stability domain of both methods. At low densities, where the chemical model is certainly applicable, numerical simulations demonstrate the formation of atoms and molecules.

To study the possibility of a phase transition in the adopted version of the chemical plasma model, we extended the model to the parameter range in which the model is unstable, using the recommendations of [15]. The numerical algorithm is based on the Newton method. The convergence of the method is provided by the requirement that the densities of all the plasma components be positive during the iteration process. If the temperature and the density (the specific volume) are chosen as thermodynamic quantities, then the requirement for the densities to be positively defined is satisfied automatically for the entire P–V diagram.

The stability of the solution was examined along the isotherm by varying the pressure or the plasma density. To search for all of the existing solutions to the set of chemical balance equations, it is convenient to move along the phase diagram from the range of high temperatures. Performing numerical calculations along different isotherms with a sufficiently small step in density, we may notice that, starting from a certain temperature, a loop appears, which is characteristic of a gas–liquid phase transition (Fig. 1). To analyze the cause of the appearance of the phase transition, we calculated isotherms for a model system consisting of only atoms and molecules (Fig. 2, curve *1*). Calculations show that the

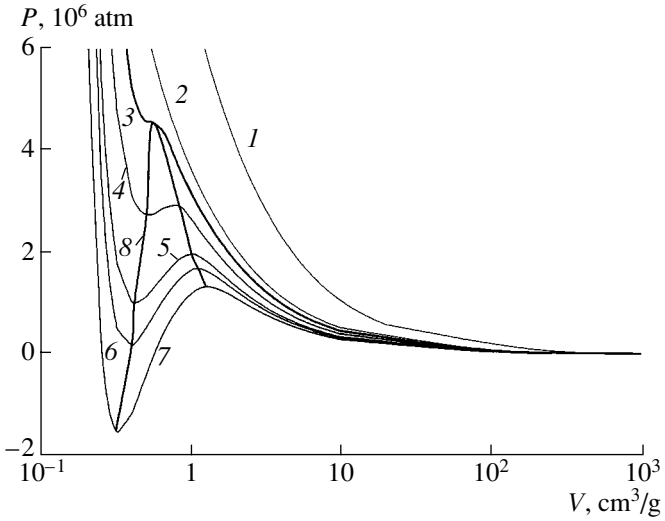

Fig. 1. Phase transition in a hydrogen plasma. Isotherms T = (*1*) 60, (*2*) 55, (*3*) 50, (*4*) 45, (*5*) 40, (*6*) 38, and (*7*) 35 kK are shown; the envelop *8* is the phase equilibrium curve (spinodal).

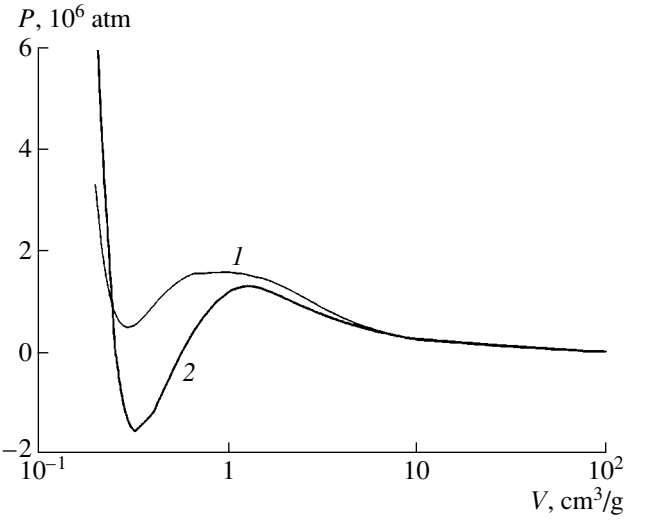

Fig. 2. Hydrogen isotherm for T = 35 kK in (*1*) the model system of atoms and molecules and (*2*) full-composition model.

main cause of the phase transition is the rapid increase in the magnitude of the total contribution from all of the second virial coefficients characterizing the pair interactions of heavy particles, which results in the intense dissociation of molecules. Taking into account all other types of particle interactions does not change the shape of the isotherm qualitatively (Fig. 2, curve *2*). In this case, the van der Waals loop becomes more pronounced. When the interaction between heavy particles is eliminated (on keeping the Coulomb interaction), the phase transition disappears. For $T < T_c$, the total second virial coefficient $B(T)$ is negative, whereas the third coefficient $C(T)$ is positive (Fig. 1, curves *4–7*). At temperatures above the critical temperature (Fig. 1, curve *3*) $B(T)$ changes its sign and the phase transition disappears (Fig. 1, curves *1*, *2*). At lower temperatures, such that $T < 1/3T_c$, the total third virial coefficient $C(T)$ is also negative. In this case, we failed to find a stable solution for the liquid phase. All the solutions lying on isotherms with $T \ll T_c$ to the left of the maximum have no physical meaning. The two-phase domain is bounded by curve *8*. The isotherm segments lying in this domain describe the states with a negative compressibility and also have no physical meaning. The value of the critical temperature for various materials is close to the dissociation energy of molecules or molecular ions.

The phase transition is accompanied by an abrupt change in the densities of all species (Fig. 3). The density jump occurs mainly due to the jump in the degree of dissociation, which allows us to call this transition the dissociative transition. It is interesting to note that the chemical model under consideration also describes an ordinary phase transition from a molecular gas into a molecular liquid at $T \sim 50$ K.

As was mentioned above, the abrupt change in the thermodynamic parameters of a hydrogen plasma was also observed in our numerical simulations using the Monte Carlo method. Figure 4 compares the analytical and simulation results. It can be seen that the model described in Section 3 not only predicts the phase transition qualitatively, but also gives a quite reasonable quantitative estimate for its position on the isotherm, which agrees with the results of numerical simulations. The obtained value of the critical temperature also agrees with the results of simulations (Fig. 4, curve *1*). The values of the internal plasma energy calculated by the chemical model and the Monte Carlo method are also in qualitative agreement (Fig. 5).

If the phase transition under consideration actually exists, then it must be accompanied by a sharp increase in the plasma conductivity, because, as is seen in Fig. 3, the density of free charge carriers in the transition point increases by three orders of magnitude. Such an increase in the electric conductivity was observed experimentally. In [1], a sharp decrease in the plasma resistivity at pressures of ~1 Mbar was recorded. A comparison of the results from calculations carried out using different models for the electron mobility shows (Fig. 6) that, at high pressures, the so-called hopping conductivity [16] shows the closest matching to the experiment:

$$\sigma_p = \frac{n_i e^2 D}{T}, \qquad (6)$$

where $D = r_p^2/\tau$ is the coefficient of the quantum diffusion of bound electrons from an atom to an ion along the applied field, $r_p = [3/4\pi(n_a + n_i)]^{1/3}$ is the average

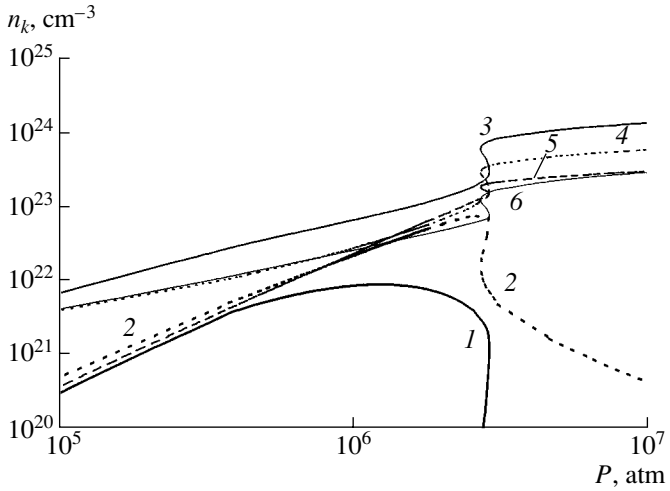

Fig. 3. Composition of a hydrogen plasma on the 45-kK isotherm: (*1*) H_2, (*2*) H_2^+, (*3*) H, (*4*) H^+, (*5*) H^-, and (*6*) e^-.

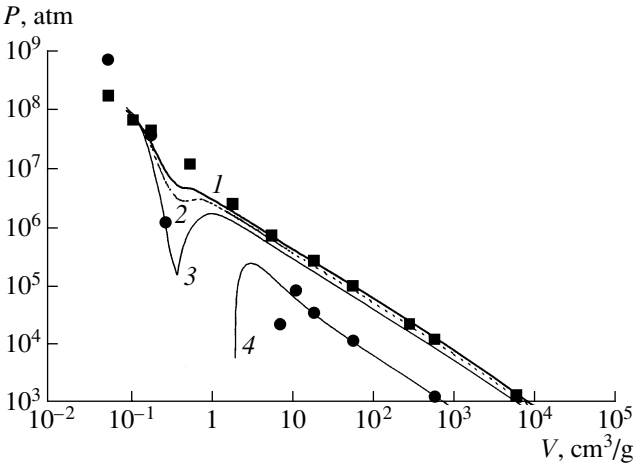

Fig. 4. Isotherms of a hydrogen plasma calculated by the chemical model for T = (*1*) 50, (*2*) 45, (*3*) 38, and (*4*) 10 kK and by the Monte Carlo method for T = 50 (squares) and 10 kK (circles).

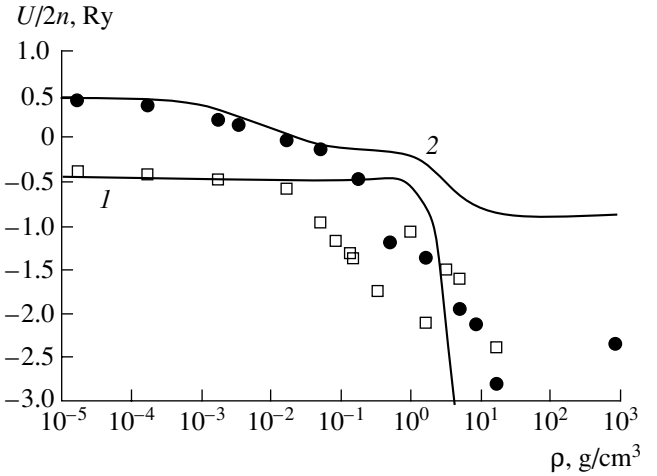

Fig. 5. Internal energy of a hydrogen plasma (U is the plasma energy per unit volume, and n is the total particle density of all species) calculated by the chemical model for T = (*1*) 10 and (*2*) 50 kK and by the Monte Carlo method for T = 10 (squares) and 50 kK (circles).

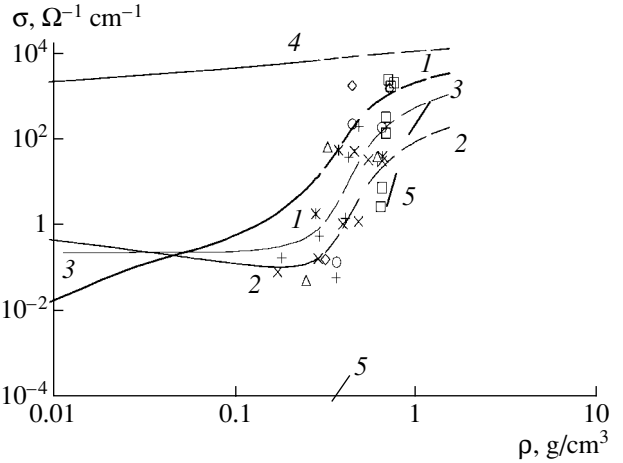

Fig. 6. Electric conductivity of a dense hydrogen plasma in the megabar pressure range along the isotherm T = 10 kK: (*1*) hopping conductivity, (*2*) gas-kinetic conductivity, (*3*) Drude formula, and (*4*) minimum metal conductivity. Curve (*5*) shows the hopping conductivity along the isotherm T = 4.5 kK, squares show the results of experiment [1], and the other symbols correspond to different experimental series of [2].

radius of the electron hopping, and $\tau = \hbar/\Delta E$ is the hopping time. According to this mechanism, the electron mobility depends on the density, because the quantity ΔE (the energy difference between the symmetric and antisymmetric terms in the A_2^+ molecule) is determined by the overlap integral for the electron wave functions [16]. Note that a sharp increase in the conductivity observed experimentally in [1] occurs at substantially (by a factor of 2.5) higher pressures than those predicted by the theory.

A large amount of experimental data is presented in [2], where a sharp increase in the electric conductivity of a hydrogen plasma was also pointed out in the density range 0.2–0.8 g/cm^3. In this case, the measured values of the plasma pressure range from 0.4 to 0.7 Mbar [2], which corresponds to the two-phase domain in Fig. 1. Consequently, the parameter range of the supposed phase transition found in our paper coincides with the range in which a rapid increase in the conductivity was observed in [2]. Although a rapid increase in the conductivity due to the abrupt change in the density and

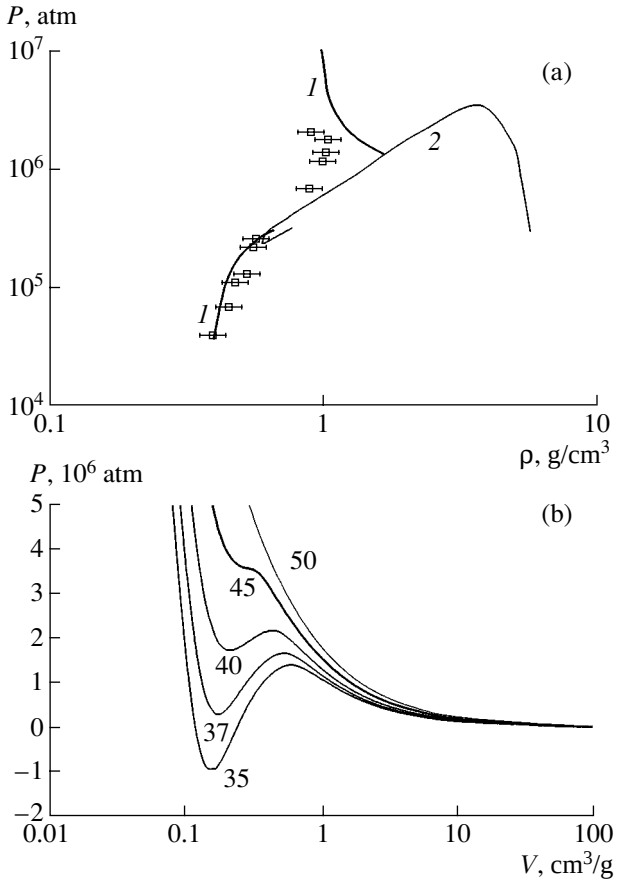

Fig. 7. Phase diagram of a deuterium plasma: (a) deuterium shock adiabat (curves *1* and *2* show the gas boundary of the two-phase domain, and squares show the results of experiment [3]) and (b) isotherms of a deuterium plasma (numerals by the curves show the temperature in kK).

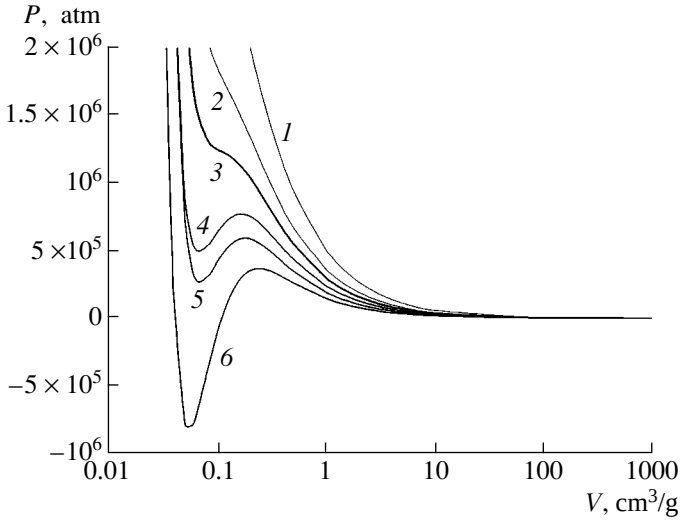

Fig. 8. Isotherms of an oxygen plasma for (*1*) 60, (*2*) 50, (*3*) 45, (*4*) 40, (*5*) 35, and (*6*) 30 kK.

composition takes place in all of the theoretical calculations, it is the hopping (ion) conduction that plays a dominant role in the dense phase (Fig. 6). The contribution from other (gas-kinetic) mechanisms is no more than 10% of the hopping conductivity. The minimum metal conductivity calculated assuming that, under the conditions of interest, all of the electrons become conduction electrons turns out to be overestimated (by nearly one order of magnitude). The bulk of the experimental data on the conductivity lies between curves *4* and *5* calculated along the 10- and 4.5-kK isotherms, respectively, which corresponds to the experimental temperature range. It should be noted, however, that all of the conductivity calculations for $\rho > 0.3$ g/cm^3 are evaluative in character, because the plasma composition in these states is calculated for unstable isotherm segments. Note also that calculations by the chemical model reliably describe only the gas–plasma branch of the isotherm. The calculations for the condensed phase are qualitative and only give estimates for the critical temperature, density, and pressure. The structure of the condensed phase (if it actually exists) can be deduced only from numerical simulations.

The anomalous behavior of thermodynamic quantities in a superdense deuterium plasma was also observed experimentally [3]. Figure 7a shows the calculated deuterium shock adiabat and the experimental results of [3]. The low-temperature branch of the shock adiabat ($T < 10$ kK) correctly describes the experimental data not only qualitatively, but also quantitatively. In addition, we observed a density jump in the adiabat near $\rho = 0.6$ g/cm^3. For $6 < T < 3.5$ kK, there is no solution to the Hugoniot adiabat equation in the gas phase. However, the calculated value of the density jump is significantly greater than the measured one. The high-temperature branch ($T > 30$ kK) of the calculated adiabat gives greatly overestimated values of the pressure at a given plasma density. This may be attributed to the scatter in the available data on the parameters of intermolecular interaction potentials for deuterium and to a significant error in the model itself near the phase transition. The proposed interpretation of the experimental data is original and nontraditional, because theoretical curves are usually continuous. The area under curve *2* in Fig. 7a determines the range of unstable solutions within the chemical model. The maximum of curve *2* (Fig. 7a) corresponds to the critical temperature $T = 4.5$ kK (Fig. 7b).

A similar behavior of the thermodynamic quantities is also observed in superdense plasmas of other molecular gases. As an example, Fig. 8 shows the phase diagram of an oxygen plasma. The critical temperature is equal to ~45 kK (curve *3*), which is close to the dissociation energy of molecular oxygen O_2^+.

5.CONCLUSION

In this study, the equilibrium properties of superdense hydrogen and deuterium plasmas in the submegabar and megabar pressure ranges have been numerically simulated by the Monte Carlo method. The same pressure range has been studied by means of the previously elaborated chemical model [10, 12, 14]. An abrupt change in the thermodynamic plasma parameters has been revealed both analytically (by using the chemical model) and numerically (by the Monte Carlo method). The mentioned features of the phase diagram can be interpreted as a phase transition of the first kind. A stepwise change in the composition and density of the medium at pressures of ~1 Mbar is accompanied by a sharp increase in the electric conductivity, which was observed experimentally in [1, 2]. It is shown that, under these conditions, the dominant charge-transfer mechanism is the quantum diffusion of bound electrons (the hopping conduction).

We can assert that the available experimental data on the shock adiabat and the conductivity of hydrogen and deuterium plasmas, together with the results of numerical simulations by the Monte Carlo method and calculations by the chemical model, suggest the existence of a new type of phase transition in dense gases. A specific feature of this transition is that the component composition changes substantially on the phase boundary between a weakly dissociated molecular gas and an atomic liquid due to the intense dissociation of molecules at a high pressure. Further compression of the liquid can lead to metallization.

ACKNOWLEDGMENTS

We are grateful W. Ebeling, M. Schlanges, A.N. Starostin, Yu.G. Krasnikov, D. Kremp, and V.S. Vorob'ev for helpful discussions and valuable remarks. This work was supported in part by the grant "School of L.M. Biberman and V.S. Vorob'ev." The work of V.S. Filinov was also supported by the NIC Jülich and the Deutsche Forschungsgemeinschaft (Mercator-Programm).

REFERENCES

1. S. T. Weir, F. C. Mitchell, and W. J. Nellis, Phys. Rev. Lett. **76**, 1860 (1996).
2. V. E. Fortov, V. Ya. Ternovoĭ, S. V. Kvitov, *et al.*, Pis'ma Zh. Éksp. Teor. Fiz. **69**, 874 (1999) [JETP Lett. **69**, 926 (1999)].
3. W. J. Nellis, A. C. Mitchell, M. van Thiel, *et al.*, J. Chem. Phys. **79**, 1480 (1983); L. B. DaSilva, P. Celliers, G. W. Collins, *et al.*, Phys. Rev. Lett. **78**, 483 (1997).
4. G. É. Norman and A. N. Starostin, Teplofiz. Vys. Temp. **8**, 413 (1970).
5. W.-D. Kraeft, D. Kremp, W. Ebeling, and G. Röpke, *Quantum Statistics of Charged Particle Systems* (Plenum, New York, 1986; Mir, Moscow, 1988).
6. D. Saumon and G. Chabrier, Phys. Rev. A **46**, 2084 (1992).
7. M. Schlanges and M. Bonitz, Contrib. Plasma Phys. **35**, 109 (1995).
8. V. S. Filinov, M. Bonitz, and V. E. Fortov, Pis'ma Zh. Éksp. Teor. Fiz. **72**, 361 (2000) [JETP Lett. **72**, 245 (2000)].
9. V. S. Filinov, V. E. Fortov, M. Bonitz, and D. Kremp, Phys. Lett. A **274**, 228 (2000).
10. I. A. Mulenko, E. N. Oleĭnikova, V. B. Soloveĭ, and A. L. Khomkin, Teplofiz. Vys. Temp. **39**, 13 (2001).
11. R. P. Feynman and A. R. Hibbs, *Quantum Mechanics and Path Integrals* (McGraw-Hill, New York, 1965; Mir, Moscow, 1968).
12. I. A. Mulenko, V. B. Soloveĭ, A. L. Khomkin, and V. N. Tsurkin, Teplofiz. Vys. Temp. **37**, 518 (1999).
13. T. L. Hill, *Statistical Mechanics: Principles and Selected Applications* (McGraw-Hill, New York, 1956; Inostrannaya Literatura, Moscow, 1960).
14. A. L. Khomkin, V. S. Vorob'ev, I. A. Mulenko, and E. N. Oleĭnikova, Fiz. Plazmy **27**, 369 (2001) [Plasma Phys. Rep. **27**, 347 (2001)].
15. V. A. Dubovitskiĭ, Yu. G. Krasnikov, and G. A. Pavlov, Fiz. Plazmy **22**, 367 (1996) [Plasma Phys. Rep. **22**, 334 (1996)].
16. *Outlines of Physics and Chemistry of Low-Temperature Plasma*, Ed. by L. S. Polak (Nauka, Moscow, 1971).

Translated by N. F. Larionova